View metadata, citation and similar papers at core.ac.uk

brought to you by CORE

provided by Digital Repository @ Iowa State University

IOWA STATE UNIVERSITY
Digital Repository

Agricultural and Biosystems Engineering Conference Proceedings and Presentations

Agricultural and Biosystems Engineering

2015

Development of an Automatic Maize Seedling Phenotyping Platform Using 3D Vision and Industrial Robot Arm

Hang Lu
Iowa State University

Lie Tang
Iowa State University, lietang@iastate.edu

Steven Whitham
Iowa State University, swhitham@iastate.edu

Follow this and additional works at: https://lib.dr.iastate.edu/abe_eng_conf


Part of the Agriculture Commons, Agronomy and Crop Sciences Commons, and the Bioresource and Agricultural Engineering Commons

The complete bibliographic information for this item can be found at https://lib.dr.iastate.edu/abe_eng_conf/562. For information on how to cite this item, please visit http://lib.dr.iastate.edu/howtocite.html.

This Conference Proceeding is brought to you for free and open access by the Agricultural and Biosystems Engineering at Iowa State University Digital Repository. It has been accepted for inclusion in Agricultural and Biosystems Engineering Conference Proceedings and Presentations by an authorized administrator of Iowa State University Digital Repository. For more information, please contact digirep@iastate.edu.

Development of an Automatic Maize Seedling Phenotyping Platform Using 3D Vision and Industrial Robot Arm

Abstract
Corp breeding plays an important role in modern agriculture, improving plant adaptability and increase yield. Optimizing genes is the key step to discover the beneficial genetic traits for crop production increasing. Associating genes and their functions needs a mountain of observation and measurement of the phenotypes, which is a dreary and fallible job for human beings. Automatic seedling phenotyping system aims at replacing the manual measurement, reduce the sampling time and increase the allowable work time. In this research, we developed an automated maize seedling phenotyping platform based on a ToF camera and an industrial robot arm. A ToF camera is mounted on the end-effector of the robot arm. The arm brings ToF camera to different viewpoints for acquiring 3D data. Camera-to-arm transformation matrix is calculated from hand-eye calibration, which is applied to transfer different viewpoint into arm base coordinate frame. Filters remove the background and noise in the merged seedling point clouds. 3D-to-2D projection and x-axis pixels density distribution method is used to segment the stem and leaves. Finally, separated leaves are fitted with 3D curves for parameter measurement. In testing experiment, 60 maize plants at early growth stage (V2~V5) were sampled by this platform.

Keywords
Phenotyping, Maize breeding, 3D reconstruction, Point clouds, robot arm, ToF camera

Disciplines
Agriculture | Agronomy and Crop Sciences | Bioresource and Agricultural Engineering

Comments
This proceeding is published as Lu, Hang, Lie Tang, and Steven Alan Whitham, "Development of an Automatic Maize Seedling Phenotyping Platform Using 3D Vision and Industrial Robot Arm," ASABE Annual International Meeting, New Orleans, LA, July 26-29, 2015. Paper No. 152189844. DOI: 10.13031/aim.20152189844. Posted with permission

This conference proceeding is available at Iowa State University Digital Repository: https://lib.dr.iastate.edu/abe_eng_conf/562

2950 Niles Road, St. Joseph, MI 49085-9659, USA
269.429.0300 fax 269.429.3852 hq@asabe.org www.asabe.org

An ASABE Meeting Presentation

Paper Number: 152189844

DEVELOPMENT OF AN AUTOMATIC MAIZE SEEDLING PHENOTYPING PLATFROM USING 3D VISION AND INDUSTRIAL ROBOT ARM

Hang Lu[1], Lie Tang[1], Steven A Whitham[2]

1 Iowa State University, Agricultural and Biosystem Engineering Department. Ames, IA, 50011, USA.
2 Iowa State University, Plant Pathology and Microbiology Department. Ames, IA, 50011, USA.

Written for presentation at the

2015 ASABE Annual International Meeting

Sponsored by ASABE

New Orleans, Louisiana

July 26 – 29, 2015

(The ASABE disclaimer is in a table which will print at the bottom of this page.)

Abstract.

Corp breeding plays an important role in modern agriculture, improving plant adaptability and increase yield. Optimizing genes is the key step to discover the beneficial genetic traits for crop production increasing. Associating genes and their functions needs a mountain of observation and measurement of the phenotypes, which is a dreary and fallible job for human beings. Automatic seedling phenotyping system aims at replacing the manual measurement, reduce the sampling time and increase the allowable work time. In this research, we developed an automated maize seedling phenotyping platform based on a ToF camera and an industrial robot arm. A ToF camera is mounted on the end-effector of the robot arm. The arm brings ToF camera to different viewpoints for acquiring 3D data. Camera-to-arm transformation matrix is calculated from hand-eye calibration, which is applied to transfer different viewpoint into arm base coordinate frame. Filters remove the background and noise in the merged seedling point clouds. 3D-to-2D projection and x-axis pixels density distribution method is used to segment the stem and leaves. Finally, separated leaves are fitted with 3D curves for parameter measurement. In testing experiment, 60 maize plants at early growth stage (V2~V5) were sampled by this platform.

Keywords. *Phenotyping, Maize breeding, 3D reconstruction, Point clouds, robot arm, ToF camera*

Introduction

Breeders, ecologists and systematisms have been studying the plant phenotyping for many years. High

The authors are solely responsible for the content of this meeting presentation. The presentation does not necessarily reflect the official position of the American Society of Agricultural and Biological Engineers (ASABE), and its printing and distribution does not constitute an endorsement of views which may be expressed. Meeting presentations are not subject to the formal peer review process by ASABE editorial committees; therefore, they are not to be presented as refereed publications. Citation of this work should state that it is from an ASABE meeting paper. EXAMPLE: Author's Last Name, Initials. 2015. Title of Presentation. ASABE Paper No. ---. St. Joseph, Mich.: ASABE. For information about securing permission to reprint or reproduce a meeting presentation, please contact ASABE at rutter@asabe.org or 269-932-7004 (2950 Niles Road, St. Joseph, MI 49085-9659 USA).

throughput phenotyping for hundreds of genotypes evaluation is routine in plant breeding (Foundation and Mcb, 2011). Ijiri et al. (2005) developed an application to model flowers in 3D. This system could figure the layout of floral components on a flower, which helped botanists concisely describe the structure of flowers quickly and easily. Some groups of researchers provided 3D models of rice plant from images and barley plant from 3D sensor. Watanabe et al. (2005) used a 3D digitizer to measure the rice plant structure in order to specify rice plant architecture and to find suitable function to describe its 3D growth at all stages. Nowadays, plant phenotyping gain more attention since the development of advanced sensors and robotic technique benefit data collecting and monitoring skills. Ulrich et al. (2011) used 3D LIDAR sensors to develop an application to deal with the detection and segmentation of plants and ground. The result showed that this application could help the agricultural robots of localization, mapping and navigation. Yann et al. (2012) proposed an algorithm based on 3D data to do plant segmentation from top view. In their experiment, the leaves of yucca and apple tree in different depth can be segmented and distinguished very well.

There are some methods for corn phenotype discovery and 3D visualization. Dornbusch et al. (2007) improved the modeling function of the shape of corn plant's leaves and stems. And a new method was proposed to parameterize the function by 3D point cloud of the plants. Although they achieved excellent results, the image cannot be captured automatically and this approach was not proved to satisfy all kinds of corn plant. De Moraes Frasson et al. (2010) also developed an application to build detailed three-dimensional digital models of corn plant by using an unmodified commercial digital camera and software. 3D reconstruction of plant is the basic of processing, which provides the morphology and position information, and the goal is to function on the plant (such as probing, cutting of the plant and so on). G. Aleny`a et al. (2011) used ToF depth data to get quadratic surface fitting which were applied in segment plant images. Their experiment result showed that the obtained surface fit well with target one and the candidate leaves could be approached by the robot-mounted camera according the location information. This work proved that combining dense color data and depth data could provide a good 3D approximation to finish plant measurement automatically.

One potential application is to use the phenotype information for guiding agricultural or biological robot. Ch.-H. Teng et al. (2011) treated normalized centroid-contour distance as the classification feature to sort different leaves in their system. Their leaf segmentation and classification system combine 3D information and color character for leaf classification, however, is not fully automatic. R. Klose et al. (2009) conducted an outdoor automatic plant phenotyping system. The conclusion gives that the ToF cameras could also be usable in outdoor field condition like direct sunlight according to experiment result. Also their system could collect the data in a movement speed of 3.6 km/h, which means it is usable in combination with an autonomous field robot.

This research is to develop a fully automatic maize seedling phenotyping platform, which is capable of output maize seedlings morphological traits, including number of leaves, leaf length, leaf angle, stem height, and plant volume.

Materials and Method

An overview of the platform is shown in Figure 1. Our system contains a time-of-flight (ToF) camera (SR_4000, MESA Imaging, Switzerland), an industrial robot am (RV_3SD, Mitsubishi, Japan), and a computer station. After pressing the "Acquire 3D data" button in the user interface, the system would send command to robot arm, including commands to specific positions with poses and to acquire a 3D point cloud with these viewpoints. Then the point clouds would be transformed and merged into arm base coordinate. The platform perform filtering, stem and leaves segmentation, phenotype output, and visualization.

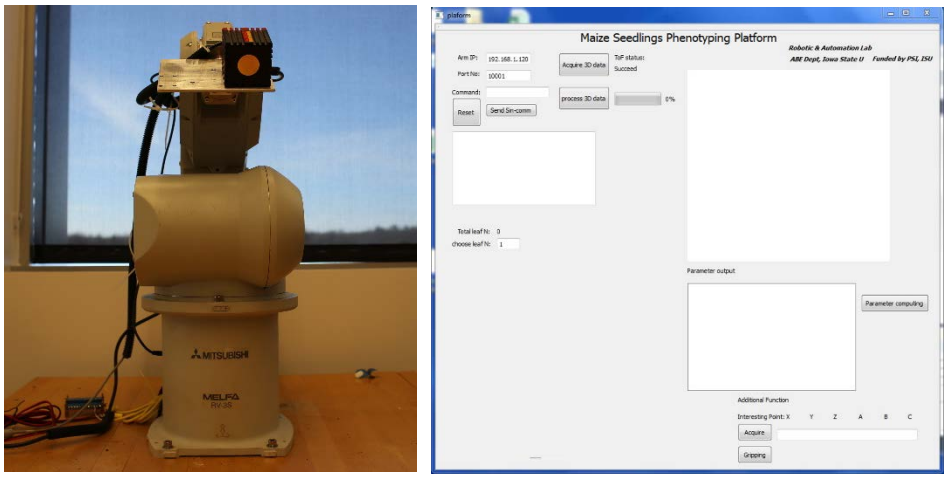

Figure 1. Hardware set-up (left) and software interface (right).

Data collection station setup

In this section, Figure 2 shows how the ToF camera connect to the end-effector of the robot arm. The aluminum mounting bracket (McMaster-CARR, USA) is 90 degree "L" shape with 5 inch width and ¼ inch depth. It was designed and machined by Manual Mills (Clausing, USA), with 4 holes on one side connecting to the robot arm end-effector, and 3 holes on the other side for fixing the ToF camera.

Figure 2. ToF camera mounted on the end-effector of the robot arm.

Hand-eye transformation matrix

In order to estimate the 3D position and orientation of the target object related to robot base coordinate frame, it is essential to know the relation between robot end-effector and robot base, between the camera and robot end-effector, and between the target object and camera. The transformation matrix between robot end-effector and base frame can be read from the robot controller output without programming or computing. The main function of the ToF camera is to output the 3D point clouds, which provides the position and orientation of target object in camera coordinate frame. Thus, the transformation matrix of camera and robot end-effector must be measured or calibrated to transfer target object position and orientation information to robot base frame.

Dimension method

The accuracy of Manual Mills that machining the mounting bracket is ±0.127 mm (±0.005 inch). According to the dimensions and coordinate definition of the ToF camera in the manual, the original point is the center of the surface and xyz direction are shown in the figure. The transformation matrix from camera xyz coordinate (Figure 3) to robot arm end-effector is calculated as represented as rotation matrix and transformation matrix.

$$R_D = \begin{bmatrix} -0.9998, 0.0174, -0.0006 \\ -0.0175, -0.9992, 0.0349 \\ 0.0000, 0.0349, 0.9994 \end{bmatrix} \quad (1)$$

$$T_D = \begin{bmatrix} -30.69 \\ -69.03 \\ 120.96 \end{bmatrix} \quad (2)$$

Fully vision-based calibration

In the normal camera calibration, there are two main outputs, intrinsic and extrinsic parameters. Intrinsic parameter is used to calibrate the lens distortion, and extrinsic parameter can be used to associate the camera position with 3D world space. Vision-based robot hand-eye calibration applies the normal camera calibration extrinsic parameters and the constant relation between camera frame and robot end-effector frame. We used Hand-Eye calibration Toolbox (Christian W, 2006) to calculate the camera to robot end-effector transformation matrix.

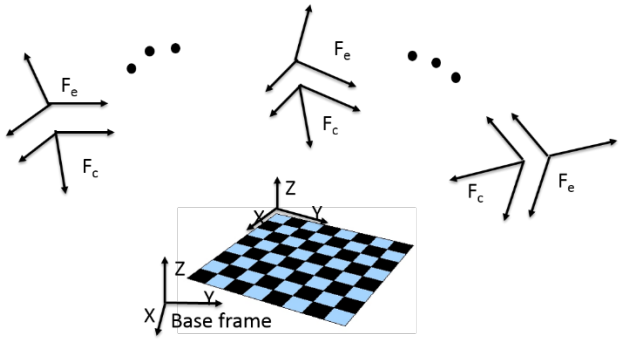

Figure 3. Hand-eye calibration, relationship between camera coordinate and robot arm base coordinate.

This toolbox would solve 8 set of homogeneous transform equations: AX=XB, where X is the unknown and target matrix. The final result of camera related to robot end-effector transform matrix had the error of 20 mm at least in each direction.

The toolbox uses the reference pattern method to locate the original and direction of the coordinate. However, this method becomes less effective when dealing with cameras with lower resolution. The reason is that the algorithm relies on the accuracy of detection of the metric features such as corner and circle center. Larger error is generated when detecting and locating those features in a low-resolution image acquired by a ToF camera, where SR_4000 only has a resolution of 176×144.

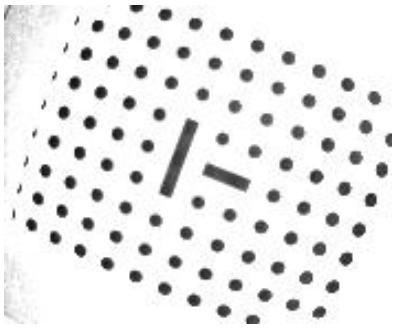

Figure 4. ToF camera amplitude image of a checkerboard with low resolution

Comparing these two calibration methods, the error of the dimension method is apparently smaller than the vision based in ToF camera case. Kahn et al (2014) reported that there is around 10mm error of SR_4000 2D and 3D image based hand-eye calibration in their experiment. Therefore, dimension method is applied in this project.

System layouts and communication

This system contains four hierarchy modules: main control module and user interface, robot arm control module, ToF camera control module, and data processing module. The entire system works as multiple threads, which the central module is the main thread and submodules are child threads, and is written in Qt development environment with program language of C++.

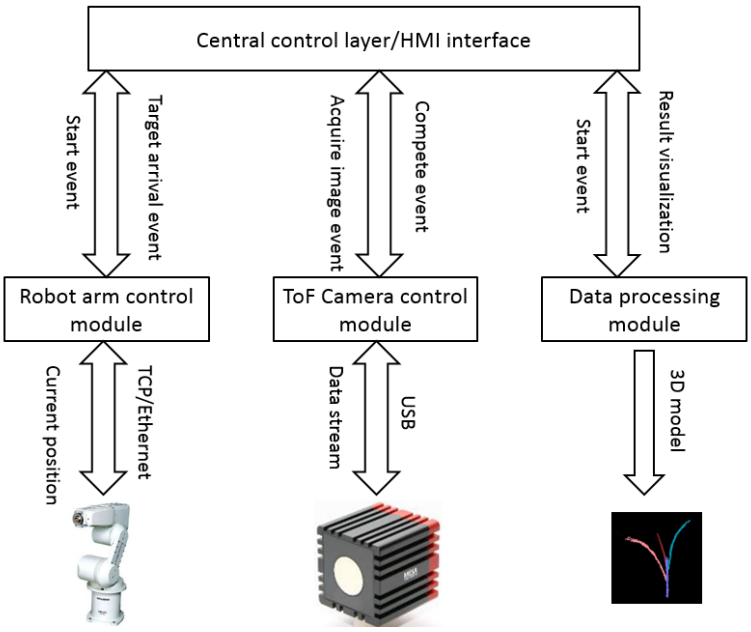

Figure 5. System overview

Main control layer

This main module and interface is a central controller which is responsible for communication with the robot arm, decision making for ToF camera action, and triggering data processing and result visualization.

According to user operation, the main control layout sends request instruction to robot arm control module. Then robot arm module would produce a program for jogging the arm to specific positions, in the meanwhile, robot arm could tell the current positon to main control module in real-time. There is a judgment whether the arm gets the target sampling position in main control module. As soon as the arm gets the target places, main control module would sends request instruction to ToF camera control module for acquiring 3D image. When the 3D images of multiple views are ready, processing module starts with filtering, leaf and stem segmentation, parameter computation. Finally, the phenotype result and 3D reconstruction model are shown as a table and zoom in/out visualization window in the user interface.

The HMI (Human-machine interaction) interface is designed friendly, with robot arm controller IP and port setting, commanding buttons, camera status checking, phenotype parameter output table, and 3D model visualization.

Robot arm control module

Mitsubishi RV3S is an industrial vertical 6-joints robot arm with maximum speed of 5.5 m/s and 0.02 mm position repeatability. The programming platform RT ToolBox2 (Mitsubishi, Japan) is an independent software with its uniform robot programming language. It is impossible to use this programming software in this project, because our system requires real-time communication, online decision-making and path planning. In this research, we applied the robot protocol and send these protocol commands to robot controller through TCP socket. The advantage of the robot protocol code is that programmers can embed the command in their customized software with other computer languages.

The robot arm controller works as a TCP server and this robot control module works as a TCP client, and they connect with Ethernet cable. In the communication mechanism, the client must open a channel by “OPEN=TOLL” command. Then it needs operation enable, turning on servo, movement programming, turning off servo and disconnection. Figure 10 shows the robot arm protocol programming structure. The robot controller returns feedbacks for every client request instruction with: Qok<Answer> or QeR<Error No.>.

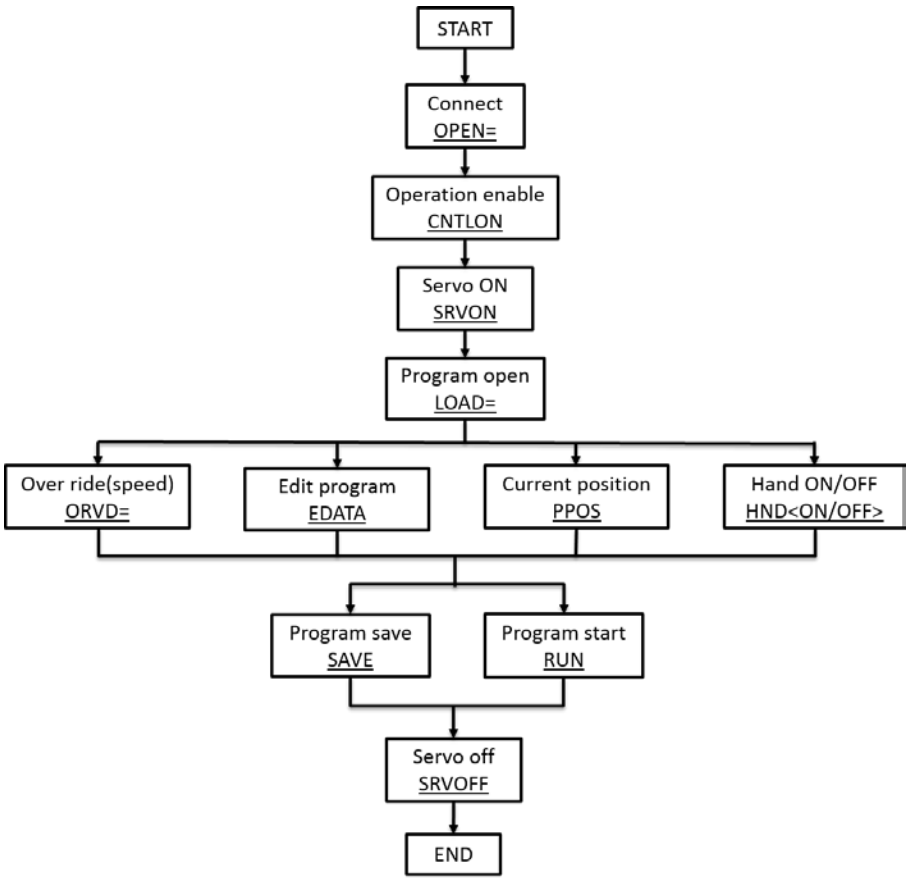

Figure 6. Robot arm programming flow chart.

ToF camera control module and data processing module

SR_4000 (MESA Imaging AG, Switzerland) is a 3D camera based on Time-of-Flight principle. The camera works as an active IR-light illumination source, and the object would reflect the IR light back to camera sensor. The camera measures the time of the light travelling between transmitting and receiving. The data output from SR_4000 is a 176×144 matrix, each element includes x, y, and z values.

The camera control module always provides a status signal to main control module as soon as the system turns on. If the two condition are satisfied: camera status is “succeed” and robot arm arrives the target positon, the central module would generate an event. The camera module triggers the sensor to acquire an image to respond this event. Calibrated out stream will be transmitted to camera module from sensor though USB. Then the data forms a “<positon No>.pcd” file in the memory and the camera module will generate an event to main module after completing image acquirement.

When the main layer respond the imaging completing event, the data processing module start to work. The details of the processing algorithm are discussed in the next chapter. Processing results will be transmitted to main module for visualization on interface.

3D image pre-processing and segmentation

Point clouds pre-processing and leaf-stem segmentation is one part of data processing module. Pre-processing contains background and noise filtering, multiple-views data merging. In leaf-stem segmentation algorithm, we firstly project 3D data into 2D z-y plane, then apply the y-axis pixels density distribution method to get stem positions in y-axis. After isolating the stem point clouds, the rest of points will be separated to several leaf clusters.

Multi-view images

In order to reconstruct more details, multi-view images are applied instead of only one from front view. Standard field of view range of SR_4000 ToF camera is 43° (horizontal) × 34° (vertical). The maize seedling is placed 550~800 mm right ahead origin of robot arm base coordinate, the distance between the center of the

sensor and plant is 800mm . The movement arrange of the robot arm is 0~859 mm independent freedom in z axis, -642~642mm independent freedom in y axis, and -330~642 mm independent freedom in x axis. In fact, the movement is limited when 6 joints works together, and the range is complex and changeable when considering the axis rotation yaw, pitch, and roll of the end-effect frame. We can treat the seedling as a cuboid model, and acquire the 3D data of its 4 facets at most. Thus, the camera should acquire images with 3 different viewpoints at least. In the left viewpoint, only left and front facets are visible for ToF camera. In the center viewpoint, the front and upper facets are visible. The right and front facets are visible from the right viewpoint.

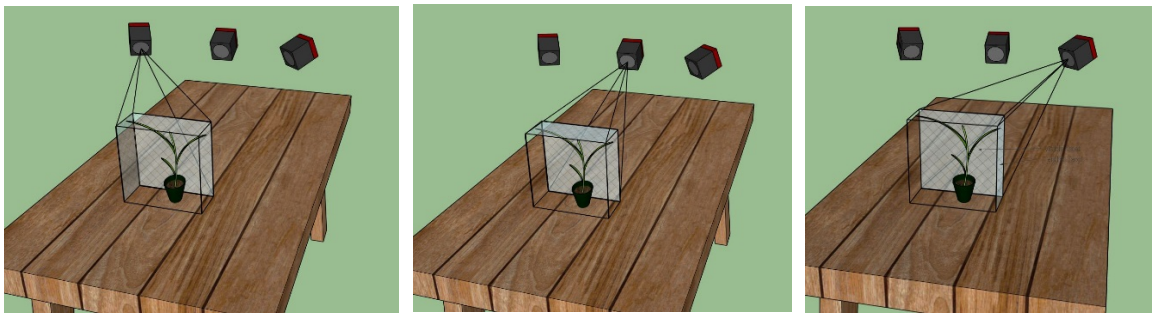

Figure 7. 3D data acquisition in multi-views.

In each viewpoint, the robot arm produces a homogenous transformation matrix to describe relationship between the end-effecter frame and robot arm base coordinate. All xyz data from different viewpoints can be transferred to base coordinate by implement this equation:

$$\begin{bmatrix} x \\ y \\ z \\ 1 \end{bmatrix}_{base} = \begin{bmatrix} x \\ y \\ z \\ 1 \end{bmatrix}_{Camera} * \left[R \mid T\right]_{cam-to-end} * \left[R \mid T\right]_{end-to-base} \quad (3)$$

Where camera to end-effector transformation matrix is calculated by calibration method, end-effector to base transformation matrix is produced by robot arm controller.

Background and noise removal

The working area is a rectangle of 250 mm length and 150 mm width in front of the origin of robot base coordinate along +x axis direction. The maximum height and width of the corn seedling are set as 600 mm and 500 mm. Then we just keep the points inside the range of the cuboid with 250 mm (width) × 500 mm (length) × 600 mm (height). Thus, the table and walls background are removed.

It is typically for a ToF to generate point cloud with varying densities. The raw data of the corn point cloud always contains a few sparsely distribution outlier points. The statistical outlier removal algorithm treats a point as outlier or inlier according to the distance to its k-nearest neighbors (Rusu et al. 2008). The threshold is set as $\mu + \beta\sigma$, where μ is the average and the σ is the standard deviation of the k neighbor distances. The k-nearest neighbors distance value of sparse points is normally greater than the threshold, $\mu + \beta\sigma$.

The value of β is the key effect on filtering result. If the β is too small, only few noise points are removed. If the value of β is too high, the points of the plant could be removed as well. We used $k = 10$ and $\beta = 10$ as the parameter in the filter (Supawadee et al. 2014).

Leaf and stem segmentation

Parameters computation and traits extraction are based on segmentation, because separated component, such as one leaf, is easier for morphology analysis. In 3D leaves and stem segmentation, Supawadee et al. (2014) slices the corn point cloud from stem bottom to leaves top, and makes least squares ellipse fitting in each module. The linked ellipses with close center and semi-major axis length are considered as stem parts. Ji (2014) projects the 3D corn point cloud into 6 binary images from 0, 60, 120, 180, 240, 300, degree view angle. If the straight line has over 50 pixels and inclination angle is from -5° to +5°, his system would treat this line as the stem.

In our segmentation algorithm, the corn point cloud is projected into a binary image. The white pixels belonging to plant are 1, the black pixels are 0 in the image. In this research, the stems of our corn plants are normally 85°~95° to ground.

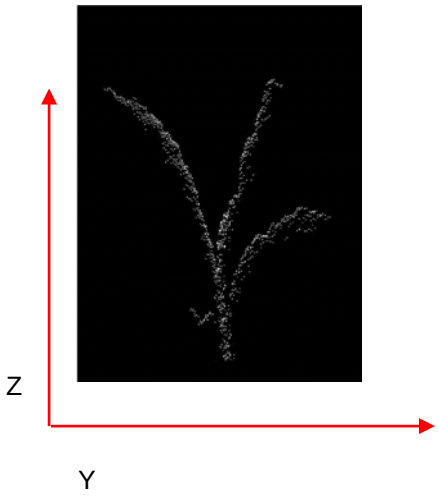

Figure 8. 2D projection binary image

Then we calculate how many white pixels there are in each unit along y direction. This is a pixels density distribution map along y axis. Because stem part is approximate vertical, it must have highest density in the distribution map. The y values of the highest density area is the location of the stem in y axis. Then the mean value of the density is μ, and standard deviation is α. We define the μ + 3×α as threshold to find the beginning (y_1) and end position (y_2) of stem in y direction. Thus point clouds of stem are separated after removing the points which are outside this interval (y_2 - y_1).

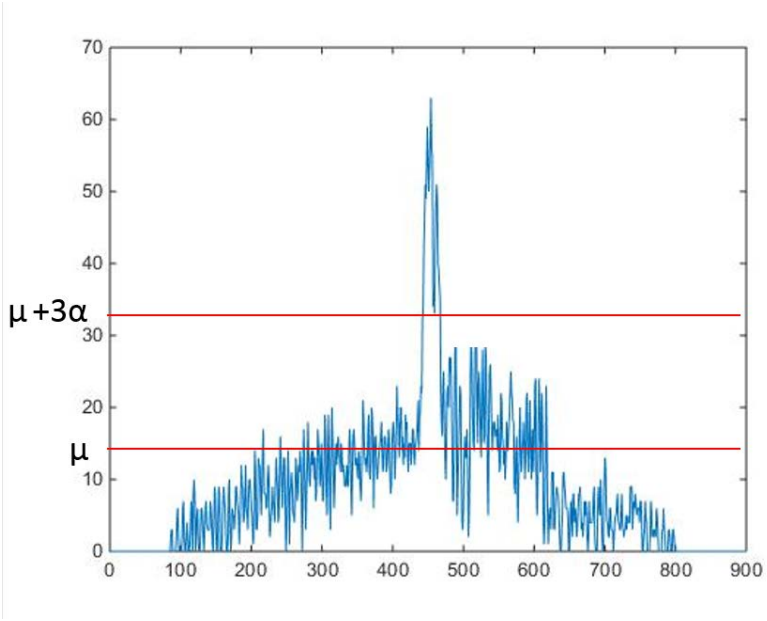

Figure 9. 2D projection binary image

After extracting the stem point cloud, the retaining points are the leaves. In order to separate the leaves points into several single ones, a clustering method called “Euclidean Cluster Extraction” (Rusu, 2009) is applied in this algorithm. The algorithm should define how a point belongs to a point cluster and what it is different from other point cluster. Let p_i, $p_j \in \mathcal{P}$, if the minimum distance from a set of points p_i to p_j is larger than the threshold d_{th}, p_j must belong to other cluster.

$$\text{Minimum} \parallel p_i - p_j \parallel \geq d_{th} \quad (4)$$

We create a kd-tree T to stand for the input leaves point cloud $\mathcal{P}$, build a list of clusters L to store the output. For every point $p_i \in \mathcal{P}$, we add it to a queue Q and search for the set p_k who is the neighbors of p_i in a sphere with radius less than d_{th}. When it is done, add the Q to the leaf cluster L_k. After traverse all p_i, the segmented leaf clusters are stored in L.

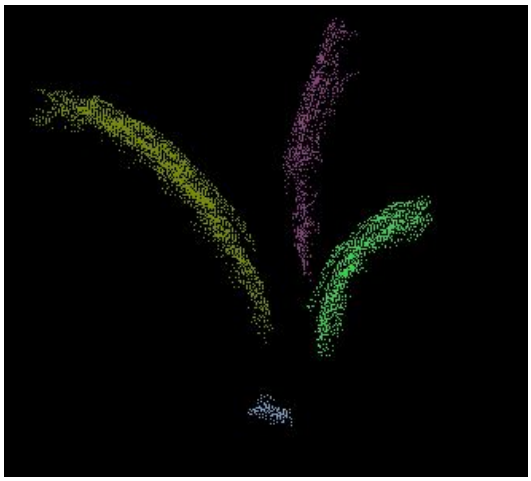

Figure 10. 2D projection binary image

Leaf curve fitting and parameter computation

Before the leaf parameters extraction, the algorithm uses a high-order 3D curve to describe the skeleton of each leaf. In the x-y plane, the skeleton of the leaf is a line. If the leaf is viewed in y-z plane, the leaf skeleton is a curve. Thus, we split the high-order 3D curve into 2 equations:

$$x = k \times y + b \tag{5}$$

$$z = \beta_0 + \beta_1 \times y + \beta_2 \times y^2 + \ldots + \beta_k \times y^k \tag{6}$$

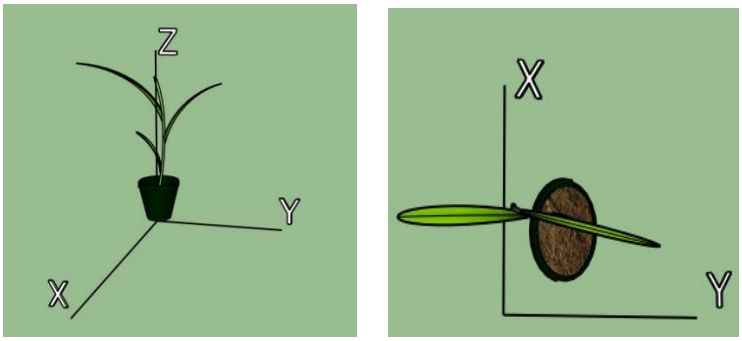

Figure 11. Right is the plant in y-z plane, left is the plant in x-y plane.

In y-z plane, the leaf skeleton with larger curvature must have larger k value. There are 97 leaves, length ranged from 50 mm to 521 mm, are chosen randomly to test which order is suitable in this project. Compared with the ground-truth, the error distribution plot and summary statistics table are show below.

$$Error = \frac{\left| system\ output - groundtruth \right|}{groundtruth} \times 100\% \tag{7}$$

The mean of error of “second order” is 0.1316, which is the smaller than first order (0.1525) and third order (0.1559). The median of the error of “second order” is the smallest. Thus we set k equal to 3 which is satisfied under most situations.

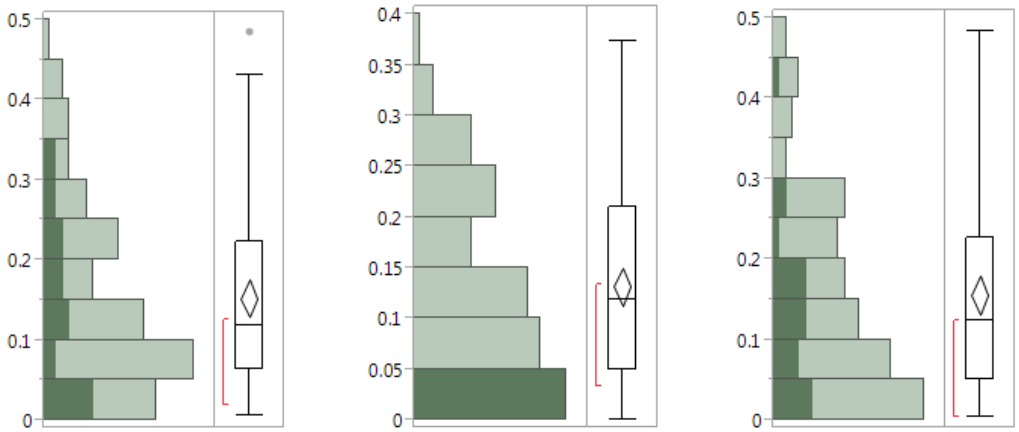

Figure 12. Leaf length error distribution with different order value. (Left is 2 order, middle is 3 order, left is 4 order)

Table 1.leaf length error estimated by different orders fitting

k = 2 (second order)			k = 3 (third order)			k = 4 (forth order)		
			Quantiles table					
100%	maximum	0.4838	100%	maximum	0.3735	100%	maximum	0.4837
75%	quartile	0.2237	75%	quartile	0.2104	75%	quartile	0.2274
50%	median	0.1188	50%	median	0.1183	50%	median	0.1236
25%	quartile	0.0641	25%	quartile	0.0499	25%	quartile	0.0509
0%	minimum	0.0060	0 %	minimum	0.0002	0 %	minimum	0.0044
			Summary statistics					
Mean		0.1524	Mean		0.1316	Mean		0.1559
Std Dev		0.1146	Std Dev		0.0907	Std Dev		0.1209
Std Err Mean		0.0116	Std Err Mean		0.0092	Std Err Mean		0.0123
Upper 95% Mean		0.1756	Upper 95% Mean		0.1499	Upper 95% Mean		0.1803
Lower 95% Mean		0.1294	Lower 95% Mean		0.1133	Lower 95% Mean		0.1316
N		97	N		97	N		97

The y range of the leaf is divided into N sub. For each y value, there are corresponding x and z, which makes up a leaf point (x, y, z). When these points are connected, the created curve is the leaf skeleton.

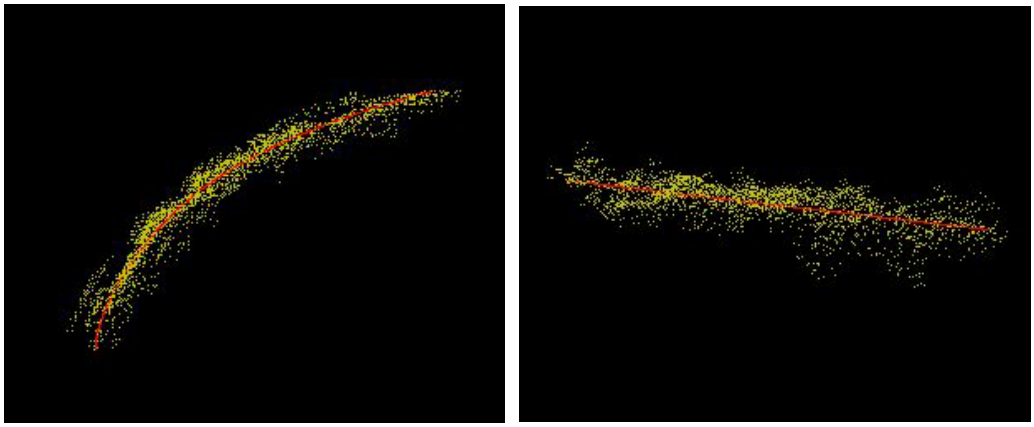

Figure 13. Right red line is the leaf fitting in y-z plane, left red line is the plant in x-y plane.

Based on the fitting curve of the leaf skeleton, the length of the leaf is the sum of N fractions length.

$$Length = \sum_{i=1}^{N} \sqrt{(x_i - x_{i-1})^2 + (y_i - y_{i-1})^2 + (z_i - z_{i-1})^2}$$

For estimation of the stem model, we fit it as a cylinder and compensate the lost bottom part due to filtering. The length of the stem is the highest z value minus the distance between desktop and bottom of the stem.

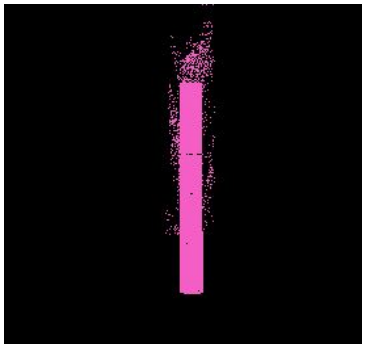

Figure 14. Stem fitting model.

Results and Discussion

After placing the plant on the working area of the desk, we power the robot arm controller and check the connection of the hardware. Then we start up the software and check the communication between the interface and ToF camera. When the status of the camera shows "succeed", we begin to operate the system.

The first step is to press the "Acquire 3D data" button. The robot arm will bring the ToF camera to different positions to collection 3D point clouds data of the plant. When the "process 3D data" bottom is pressed, the software will process the data collected above. After the process bar shows 100%, the reconstructed corn plant model will be displayed in a black window, user can then rotate it and zoom it in/out. Stem and different leaves will be labeled with different colors. In the meantime, a table will display the parameters of the plant, such as the lengths of each leaf and the stem height.

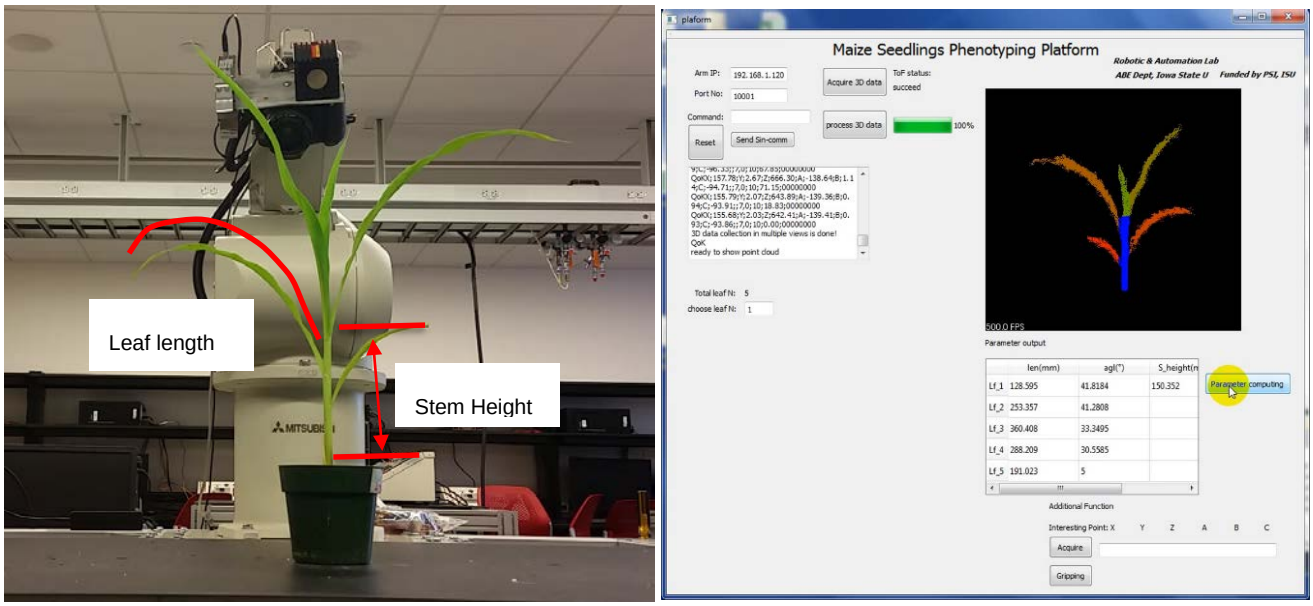

Figure 15. Working area (left) and Parameter output in the user interface (right).

We choose 60 maize plants as the experiment objects. They grows in the growth chamber, we start to measure in 7 days after they sprout. Every 3 days, we take a measurement of the plants by the system, in the meanwhile, the plants are measured by hand. The measured parameters are including stem height, and leaf length. The result measured by hand are treated as ground-truth. We take 9 times testing from the plants' 8th, 11th, 14th, 17th, 20th, 23rd, 26th, 29th, 32nd days. There are 534 stem height are measured (2 plants are dead in 29th, and 2 plants are dead in 32nd days), 1969 leaves totally are tested during this experiment.

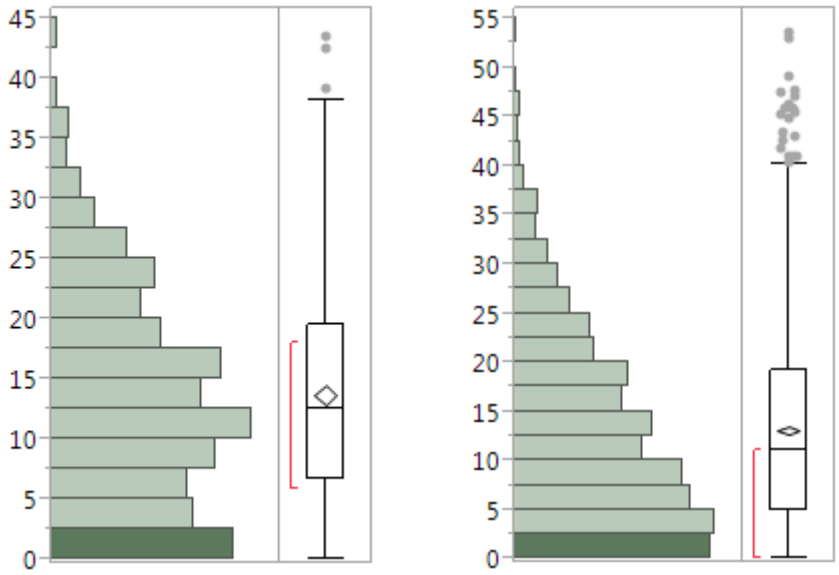

Figure 16. Error (%) distribution of the stem height (right) and leaf length (left) system measurement

Table 2. Stem height Error table (%)

Quantiles			Summary Statistics	
100%	maximum	43.5500	Mean	13.6721
75%	quartile	19.4917	Std Dev	8.9439
50%	median	12.5129	Std Err Mean	0.3870
25. %	quartile	6.6000	Upper 95% Mean	14.4325
0%	minimum	0.0166	Lower 95% Mean	12.9119
			N	534

Table 3. Leaf length Error table (%)

Quantiles			Summary Statistics	
100%	maximum	53.5031	Mean	13.0979
75 %	quartile	19.1725	Std Dev	9.8813
50%	median	11.0794	Std Err Mean	0.2227
25%	quartile	5.0017	Upper 95% Mean	13.5345
0 %	minimum	0	Lower 95% Mean	12.6611
			N	1969

The stem heights of these corn plants are ranged from 30 mm to 220 mm, the length of the leaves are ranged from 20 mm to 567 mm. The tables show that the error of stem height is 12.5129% (median value) and 13.6721% (mean value). The leaf length measurement error is 11.0794 %(median value) and 13.0979 %(mean value). The error comes from the ToF camera (10 mm), filtering, and leaf curve fitting. The parameter of filters and the order of fitting curve is difficulty to choose, because every plant has different shaped leaves. The surface of corn leaf is not flat, the fluctuated part of the leaf has large densities. Some leaf are more bent than others, so it needs more than 3-order to present the skeleton.

Conclusion

In this project, the results of phenotype extraction for maize seedlings have demonstrated the feasibility of this automatic phenotyping system. Three sources make the contributions to the error: filters, ToF accuracy and curve fitting algorithm. The current system only consider the shape of the plant, besides measuring the plants'

morphology characters, there are several of phenotyping traits we care about. It requires different sensors, such as color camera, to observe the texture changing of the leaf.

In future work, we will execute probing on the plant based on the 3D model of the seedlings. We also want to mount a 2D camera on the end-effector of the robot arm to acquire the leaf's color traits. We will need to test the system on a wider range of corn plant growth stages and try to follow the growth of seedlings.

Acknowledgments

This project is funded by: Plant Science Institute (PSI) Innovative Grant (2013-2015), Iowa State University.

References

Dornbusch, T., Wernecke, P., Diepenbrock, W., 2007. A method to extract morphological traits of plant organs from 3D point clouds as a database for an architectural plant model. Ecological Modeling 200, pp. 119-129.

De Moraes Frasson, R.P., Krajewski, W.F., 2010. Three-dimensional digital model of a maize plant. Agricultural and Forest Meteorology 150, pp. 478-488.

Ijiri, T., Owada, S., Okabe, M., Igarashi, T., 2005. Floral diagrams and inflorescences: interactive flower modeling using botanical structural constraints, in: ACM Transaction on Graphics (TOC), ACM, and New York, NY, USA. pp. 720-726.

Ulrich Weiss, Peter Biber, Plant detection and mapping for agricultural robots using a 3D LIDAR sensor, Robotics and Autonomous Systems, Volume 59, Issue 5, May 2011, pp. 265-273.

Watanabe, T., Hanan, J.S., Room, Peter M.and Hasegawa, T., Nakagawa, H., Takahashi, W., 2005. Rice morphogenesis and plant architecture: Measurement, specification and the reconstruction of structural development by 3d architectural modeling. Annals of Botany, pp. 1131-1143.

Yann Chéné, David Rousseau, Philippe Lucidarme, Jessica Bertheloot, Valérie Caffier, Philippe Morel, Étienne Belin, François Chapeau-Blondeau, On the use of depth camera for 3D phenotyping of entire plants, Computers and Electronics in Agriculture, Volume 82, March 2012, pp. 122-12.

G. Aleny`a, B. Dellen and C. Torras, 3D modelling of leaves from color and ToF data for robotized plant measuring, 2011 IEEE International Conference on Robotics and Automation [1050-4729] Alenya, G yr:2011 pg:3408 -3414.

G. Feng, C. Qizin, and M. Masateru, "Fruit detachment and classification method for strawberry harvesting robot", International Journal of Advanced Robotic Systems, vol 5, pp. 41-48, 2008.

Ch.-H. Teng, Y.-T. Kuo, and Y.-S. Chen, "Leaf segmentation, classification, and three-dimensional recovery from a few images with close viewpoints". Optical Engineering 50(3), doi:10.1117/1.3549927, 2011.

R. Klose, J. Penlington and A. Ruckelshausen: "Usability study of 3D Time-of-Flight cameras for automatic plant phenotyping", Workshop on Computer Image Analysis in Agriculture, pp. 93-105, August 2009.

Foundation, N. S., and G. Mcb. Phenomics: Genotype to Phenotype A report of the Phenomics workshop sponsored by the USDA and NSF, 2011.

Kahn, Svenja; Haumann, Dominik; Willert, Volke. "Hand-eye calibration with a depth camera: 2D or 3D", International Conference on Computer Vision Theory and Applications (VISAPP), pp.481-489, 2014.

Rusu, R.B., Cousins, S., 2011. 3D is here: Point Cloud Library (PCL), in: IEEE International Conference on Robotics and Automation (ICRA), Shanghai, China. pp. 1-4.

Supawadee Chaivivatrakul, Lie Tang, Matthew N. Dailey, Akash D. Nakarmi, Automatic morphological trait characterization for corn plants via 3D holographic reconstruction, Computers and Electronics in Agriculture, Volume 109, November 2014, Pages 109-123, ISSN 0168-1699, http://dx.doi.org/10.1016/j.compag.2014.09.005.

Ji Li. (2014). 3D machine vision system for robotic weeding and plant phenotyping. PhD dissertation, Iowa State University, USA.

Radu Bogdan Rusu. (2009). Semantic 3D Object Maps for Everyday Manipulation in Human Living Environments. PhD dissertation, Technischen Universität München, Germany.

Christian Wengert. , Mireille Reeff, Philippe C. Cattin, Gábor Székely. "Fully Automatic Endoscope Calibration for Intraoperative Use" Bildverarbeitung für die Medizin Informatik aktuell 2006, pp 419-423